Chinese Chemical Letters 34 (2023) 108586

Contents lists available at ScienceDirect

Chinese Chemical Letters

journal homepage: www.elsevier.com/locate/cclet

Facile construction of a water-defendable Li anode protection enables rechargeable Li-O_2 battery operating in humid atmosphere

Shan Min[a], Xiaoyu Liu[a], Aonan Wang[a], Fanghua Ning[a], Yuyu Liu[a], Jiaqian Qin[b], Jiujun Zhang[a], Shigang Lu[a], Jin Yi[a,*]

[a] Institute for Sustainable Energy/College of Sciences, Shanghai University, Shanghai 200444, China
[b] Metallurgy and Materials Science Research Institute, Chulalongkorn University, Bangkok 10330, Thailand

ARTICLE INFO

Article history:
Received 25 March 2023
Revised 2 May 2023
Accepted 17 May 2023
Available online 2 June 2023

Keywords:
Li-O_2 battery
Hydrophobic
Li anode protection
Humid atmosphere
Cycling stability

ABSTRACT

The rechargeable Li-O_2 battery endowed with high theoretical specific energy density has sparked intense research interest as a promising energy storage system. However, the intrinsic high activity of Li anode, especially to moisture, usually leads to inferior electrochemical performance of Li-O_2 battery in humid environments, hindering its widespread application. To settle the trouble of poor moisture tolerance, fabricating a water-proof layer on the Li-metal anode could be an effective tactic. Herein, a facile strategy for constructing an ibuprofen-based protective layer on the Li anode has been proposed to realize highly rechargeable Li-O_2 battery in humid atmosphere. Due to the *in-situ* reaction between ibuprofen reagent and metallic Li, the protective layer with a thickness of ~30 μm has been uniformly deposited on the surface of Li anode. Particularly, the protective layer, consisting of a large amount of hydrophobic alkyl group and benzene ring, can significantly resist water ingress and enhance the electrochemical stability of Li anode. As a result, the Li-O_2 battery based on the protected Li anode achieves a long cycle life of 210 h (21 cycles at 1000 mAh/g, 200 mA/g) in highly moist atmosphere with relative humidity (RH) of 68%. This convenient and efficient strategy offers novel design concept of water-resistant metal anode, and paves the way to the promising future prospect for the high-energy Li-O_2 battery implementing in the ambient atmosphere.

On account of the high theoretical specific energy density, the Li-O_2 battery has gained considerable attention as an appealing energy storage system [1–10]. However, the further development of Li-O_2 battery has been limited by the unsatisfied electrochemical performance when it is operated in ambient air. Different from dry O_2 atmosphere, the side reactions involving Li metal anode are mainly derived from the adverse effects of H_2O under humid conditions, overshadowing the widespread application of Li-O_2 battery [11–17]. For example, when the electrolyte contains tiny amounts of water, the electrochemical reaction of Li^+ with oxygen could be altered, resulting in an increase of battery capacity. Moreover, the discharge product can be converted from Li_2O_2 to soluble HO_2^-, which can reduce the polarization during the initial charge. However, the presence of H_2O adversely affects the interfacial behavior of the Li-O_2 battery during discharge/charge processes [18,19]. The water in the electrolytes or air would result in the further deteriorated side reactions, which lead to the increased interface resistance and the unfavorable cycle stability [20]. For practical Li-air batteries operating in humid ambient air, the crossover of H_2O toward active Li metal can produce intense exothermic reaction, which inevitably leads to the irreversible Li consumption and serious safety issues [21]. Until now, vast strategies, including coating treatment, alternative anode and electrolyte additive, have been proposed to suppress the detrimental effects of water [22]. Various anode materials including Si, Sn and Al-carbon, have been proposed for Li-air batteries [23–28]. The modification of cathode materials is also one of appealing strategies to suppress the attack caused by H_2O in air for Li-O_2 battery, such as constructing oxygen selective membrane on the cathode [29,30]. In addition, it is reported that the issues of parasitic reactions can be solved by the synergistic effect of 2,5-di–*tert*–butyl–1,4-benzoquinone and H_2O in a nonaqueous Li-O_2 battery [31]. Nevertheless, the electrochemical performances of Li-O_2 batteries in humid O_2 atmosphere are still far from practical applications [32]. It is well known that the Li metal would be rapidly corroded with the presence of water, leading to the degraded reversibility of Li anode and the poor stability of Li-O_2 battery (Scheme 1a). Fortunately, the above

* Corresponding author.
E-mail address: jin.yi@shu.edu.cn (J. Yi).

https://doi.org/10.1016/j.cclet.2023.108586
1001-8417/

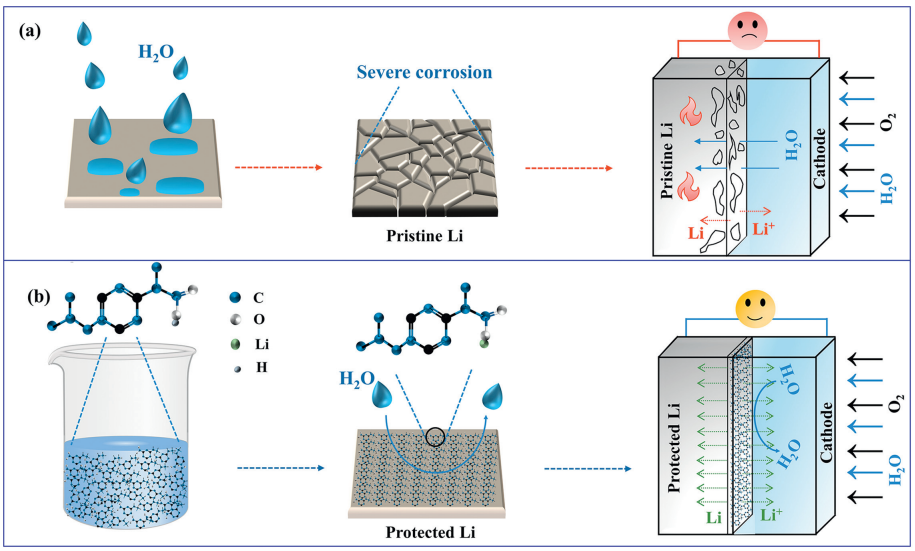

Scheme 1. The schematic of Li-O_2 battery in humidity atmosphere with: (a) pristine Li, (b) water-defendable protected Li based on the protective layer.

issue can be alleviated through employing a protective layer on the surface of Li anode, which is able to prevent water from corroding Li anode [33–37]. Inspired by the water-resistant effect of the umbrella cloth, Zhang *et al.* have decorated hydrophobic SiO_2 nanoparticles into the protective layer to block moisture invasion towards the Li anode, and finally achieved a safe and long-life Li-air battery in ambient air [38]. Zhou *et al.* have proposed a super-hydrophobic quasi-solid electrolyte consisting of SiO_2 matrix and Li-conductive ionic liquid (IL) for developing a feasible Li-O_2 battery operating in the humid O_2 environment [39]. Liao *et al.* have pretreated Li anode with $GeCl_4$-tetrahydrofuran (THF) reagent to form a Germanium-based protective layer, enabling reversible electrochemical behavior of Li anode in water-containing electrolytes and humid atmosphere with RH of 45% [40]. Therefore, preparing a hydrophobic surface layer for water-resistant Li anode has been regarded as a feasible strategy to ensure the safe and long cycle life of Li-O_2 battery in high-humidity environment [41–48]. Besides the inorganic species, the organics with hydrophobic groups also show a great potential in the protection of Li-O_2 battery from water corrosion [49]. For example, Yu *et al.* have synthesized a highly conductive polyaniline (PANI) membrane as the waterproof layer, which could reduce the evaporation of electrolyte and improve the reversibility of Li anode [50].

A polyurethane film has also been proposed to protect Li metal anode from interface destabilization derived from the crossover of water [33]. Sun *et al.* have prepared a protective layer by mixing polydimethylsiloxane (PDMS) and perfluorotributylamine (FTBA), which limits the diffusion behavior of water molecules [51]. Accordingly, the established dense and firm protective layer would hamper the water-related issues [6,52]. However, the preparation processes for the above-mentioned protective layer are complicated or expensive, which are difficult to achieve widespread application. Additionally, even though the fabricated protective layer exhibits hydrophobicity, it is still challenging to ensure the stable operation of Li-O_2 batteries under high humidity conditions.

Herein, with the aim to enable Li-O_2 battery operating in humid atmosphere, a facile and scalable strategy has been proposed to overcome the water-related issues, in which a water-defendable protective layer is artificially fabricated via the chemical reaction between Li anode and ibuprofen. Owing to the characteristic molecular structure of ibuprofen (the alkyl and phenyl groups are hydrophobic while the carboxyl group is lithophilic), the designed protective layer can be uniformly fabricated on the Li anode surface to resist water ingress. Therefore, the Li-O_2 battery with the protected Li anode exhibits a long life span of 210 h in a humid O_2 environment with relative humidity (RH) as high as 68%. As a proof of concept, the obtained findings have provided a feasible strategy to construct water-proof Li anodes for the further development of Li-air battery in ambient air.

Comparing to the other compounds with the functional group of benzoic acid, the molecular structure of ibuprofen contains alkyl groups, emerging higher hydrophobicity. In addition, the insolubility of ibuprofen in organic solvent (triethylene glycol dimethyl ether, TEGDME) has been confirmed before it is used as protective layer (Fig. S1 in Supporting information). The schematic of the Li-O_2 battery with a protective layer operating in humid O_2 atmosphere is illustrated in Scheme 1b. Ibuprofen, whose molecular structure is shown in a schematic diagram, has been reported to be almost insoluble in water [53]. Based on the chemical reaction of Li and ibuprofen, the protective layer is formed spontaneously on the surface of Li metal anode. The involved reaction is listed as Eq. 1:

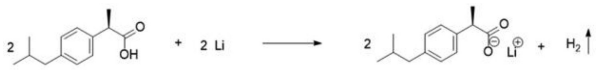

(1)

The above reaction could be demonstrated by Fourier transform infrared spectroscopy (FTIR), as depicted in Fig. 1a. The presence of unsaturated C–H bonds in phenyl corresponding to strong and wide absorption peak at around 3000 cm^{-1}, as well as C=C bonds at the fingerprint region, is found for both the pristine ibuprofen reagent (blue line) and the newly-formed protective layer (green line). After reaction with Li metal, as clearly observed in the enlarged region, the characteristic absorption peak at 1720 cm^{-1} (blue line) has been red-shifted to 1580 cm^{-1} (green line), which could result from conversion from carboxylic acid group to carboxylate ion [54]. Therefore, the *in-situ* formation of the protective layer is viable due to the spontaneous chemical reaction of ibuprofen reagent and Li anode. The morphology of the *in-situ* formed protective layer is characterized by scanning electronic microscope (SEM). It can be observed that in comparison with a smooth surface for the pristine Li anode (Fig. 1b), the protective layer newly-formed on the Li metal surface is composed of interlaced nanorod-shaped deposits with the length of approximately

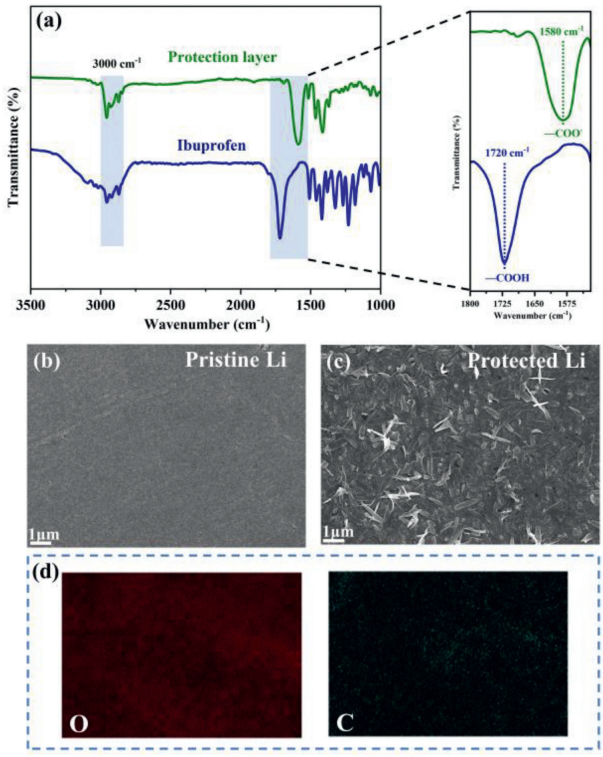

Fig. 1. (a) FTIR spectra of the pristine ibuprofen and the *in-situ* formed protective layer. The SEM image of Li anode: (b) The pristine Li and (c) the protected Li. (d) EDS mapping analysis of the protective layer.

1 μm (Fig. 1c). The result of energy dispersive spectroscopy (EDS) elemental mapping shows that the protective layer is composed of C and O with uniform distribution (Fig. 1d). Additionally, a textured surface structure can also be identified in the corresponding cross-sectional image and the thickness of the protective layer is measured as ~30 μm (Fig. S2 in Supporting information). Actually, the thickness of the protective layer can be increased by increasing the amount of ibuprofen reagents (Figs. S3a-c in Supporting information), which is corresponding to the growth of the resistance in Li-O_2 batteries (Fig. S3d in Supporting information). Although the lowest impedance has been exhibited by the Li-O_2 battery with protective layers of 20 μm thickness, it can be found the inferior waterproof of that due to its poor density on Li metal surface. These results could further confirm the uniform deposition of protective layer through the utilization of ibuprofen reagent.

In order to investigate the effects of the protective layer on the Li anode, Li-O_2 batteries were fabricated with both pristine and protected Li anodes. Firstly, the electrochemical performance of Li-O_2 batteries were tested in dry O_2 atmosphere at a current density of 500 mA/g with a fixed capacity of 1000 mAh/g. Fig. 2a shows the voltage profiles of the initial cycle for both batteries. As depicted from the curves, the total polarization voltages of the Li-O_2 batteries with pristine and protected Li anode are 1.61 V and 1.76 V, respectively. The slightly elevated overpotential of the protected Li-O_2 battery could be ascribed to the enlarged internal resistance stemming from the restricted Li^+ migration across the protective layer [49]. After 300 cycles, the terminal voltage of the pristine Li-O_2 battery gradually falls to the cut-off voltage (2.0 V), along with the obviously declined discharge capacity of 379 mAh/g (Fig. 2b). This variation reveals the dramatic increase of internal resistance in the pristine Li-O_2 battery, which could be ascribed to the onset of various side reactions and accumulation of "dead Li" upon long cycles [55]. As for the protected Li-O_2 battery, the terminal voltages of discharge/charge processes can be remained for 350 cycles with-

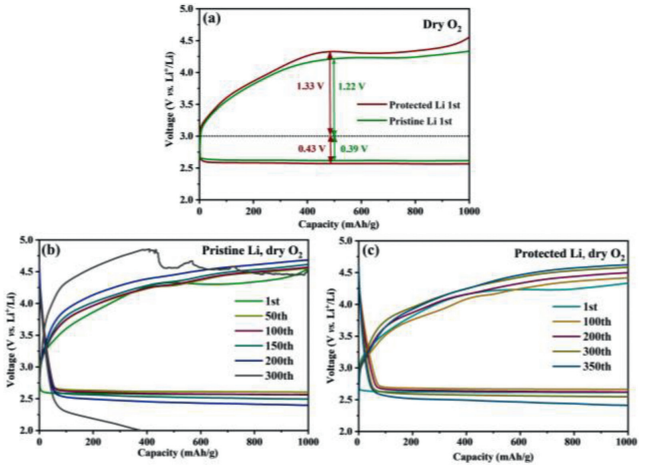

Fig. 2. Electrochemical performance of the Li-O_2 batteries using the pristine Li anode and protected Li anode in dry O_2: (a) Voltage profiles of the initial cycle; distinct discharge/charge curves of the Li-O_2 batteries using the (b) pristine Li anode and (c) protected Li anode.

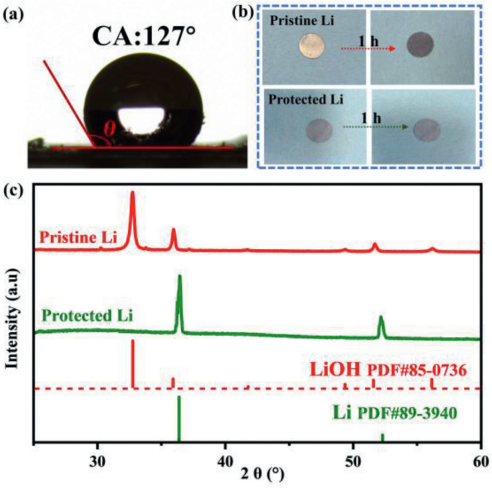

Fig. 3. (a) Contact angle of H_2O on the protective layer. (b) The optical photographs of the Li metals before and after exposing in moist air: the pristine Li metal and the protected Li metal. (c) Corresponding XRD patterns of the above Li metals after exposing 1 h in moist air.

out significant increase of overpotentials (Fig. 2c). Therefore, it can be speculated that the *in-situ* formed protective layer plays a vital role in mitigating side reaction at the interface [56]. Additionally, the corresponding voltage-time curves (Fig. S4 in Supporting information) show a favorable electrochemical stability of the protected Li anode with more than 400 h at a current density of 3 mA/cm^2 with a specific capacity of 3 mAh/cm^2, highly superior to the performance of pristine Li anode. According to these results, the uniform and reversible Li stripping/plating behavior can be achieved with the assistance of ibuprofen-based protective layer [57–62].

The hydrophobicity of the fabricated protective layer is determined through the wettability test using contact angles. As illustrated in Fig. 3a, a drop of water is placed on the surface of this protective layer, and a large water contact angle of 127° indicates the hydrophobic property of the protective layer. Thus, this hydrophobic surface layer can retard H_2O ingression toward the anode, enable to long stability of the Li anode under humid conditions. Additionally, in order to elucidate the waterproof effect of the hydrophobic protective layer, both the pristine and the protected Li anodes are exposed to moist air for comparison. As shown in Fig. 3b, after exposing 1 h in moist air, the surface of the

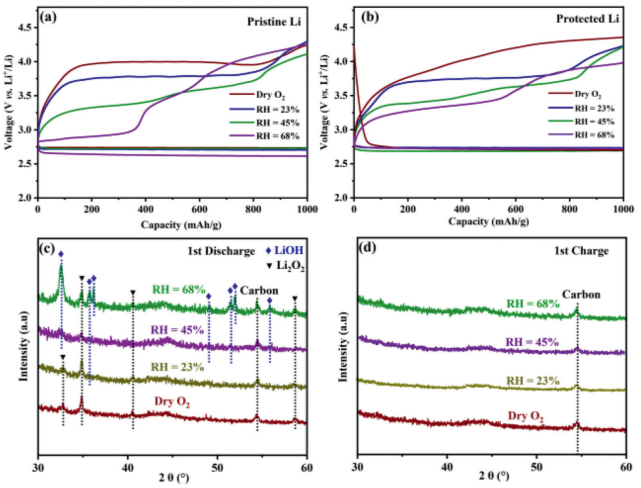

Fig. 4. The initial discharge/charge curves of Li-O_2 batteries based on (a) pristine Li anode and (b) protected Li anode under different RH. XRD patterns of the super P cathode in unprotected Li-O_2 battery after (c) discharge and (d) charge, respectively, under various RH: dry O_2, RH = 23%, RH = 45% and RH = 68%.

protected Li metal remains unchanged whereas the pristine Li surface with metallic color turns to dark gray, due to a serious corrosion of the Li metal. These results are consistent with the X-ray diffraction (XRD) patterns of the above pristine/protected Li metals after exposure (Fig. 3c). It can be found that the pristine Li metal would react with moisture in air to form the coating LiOH phase on the surface, while the additional impurity is absent for the protected Li metal, indicating the significant water-defendable effects of the ibuprofen-based protective layer in blocking side reaction under humid atmosphere. Owing to the significant role of the designed protective layer in preventing detrimental reaction of moisture with Li metal anode, the operation of the Li-O_2 battery in humid atmosphere could be expected.

To evaluate the practical application of the designed water-defendable Li anode, the symmetrical Li cells based on 1000 ppm H_2O-containing electrolyte have been investigated. As displayed in Fig. S5a (Supporting information), it can be found that the symmetrical Li cell employing the protected Li anode exhibits stable voltage-time profiles with small overpotentials, while the symmetric Li cell with the pristine Li electrode displays the instable voltage and the increased overpotentials over cycling time. Meanwhile, Figs. S5b and c (Supporting information) show the cyclic performance for the pristine and protected Li-O_2 batteries with 1000 ppm H_2O-containing electrolyte, respectively. It can be seen that the Li-O_2 battery with the protected Li anode delivers improved cyclic stability. Furthermore, the electrochemical tests of Li-O_2 batteries were conducted in O_2 atmosphere with different humidities. All the batteries are implemented at a current density of 200 mA/g with the limited capacity of 1000 mAh/g. As illustrated in Figs. 4a and b, the polarization during the initial cycle gradually decreases with the increase of humidity for both pristine and protected Li-O_2 battery. The unique electrochemical behavior could be ascribed to the distinct reaction pathway under different humidities. It has been reported that the consumption of intermediate product hydroperoxide (HO_2^-) in electrochemical reactions is beneficial to suppressing the detrimental side reactions associated with peroxide, leading to the decreased overpotential [18,20]. This could be responsible for the decreases of overpotential of Li-O_2 batteries with increasing humidity. Generally, the discharge/charge processes in non-aqueous Li-O_2 batteries are based on the reversible formation/decomposition of Li_2O_2, and the corresponding electrochemical reaction can be expressed as below (Eq. 2):

$$2Li^+ + 2e^- + O_2 \leftrightarrow Li_2O_2 \left(E^\Theta = 2.96\,V\,vs.\,Li^+/Li\right) \quad (2)$$

Nevertheless, the novel products could be formed during discharge with the presence of moisture. Figs. 4c and d present the XRD spectra of the products at the cathode after the initial discharge and charge processes in the unprotected Li-O_2 batteries under various RH conditions, respectively. Under dry O_2 atmosphere, Li_2O_2 is the sole product at the end of discharge process and vanished after subsequent charge process, which is in line with the above reaction mechanism (Eq. 2). Furthermore, the results of X-ray photoelectron spectroscopy (XPS) further reveal the sole discharge product of Li_2O_2 (54.5 eV) under dry atmosphere (Fig. S6a in Supporting information). Due to the increase of humidity, the discharge product of Li_2O_2 on the electrode surface is gradually converted to LiOH. Therefore, the intense peak corresponding to LiOH (55.5 eV), is generated after discharge at various humid conditions (Figs. S6b-d in Supporting information), indicating the altered reaction mechanism in the presence of a certain amount of water. According to XRD patterns in Fig. 4c, Li_2O_2 is still the main discharge product under low-humidity condition (RH = 23%), coexisting with a small amount of LiOH byproduct. Therefore, the formation of LiOH could result from further chemical reaction of partial Li_2O_2 discharge products with water at the surface (Fig. 4c). The abovementioned reaction mechanism can be expressed as Eq. 3:

$$2Li_2O_2 + 2H_2O \rightarrow 4LiOH + O_2 \quad (3)$$

However, under high-humidity conditions (RH = 45% and 68%), XRD patterns of discharge products mainly consist of LiOH peaks, accompanied with a tiny amount of Li_2O_2 phase. Subsequently, the newly-formed LiOH/Li_2O_2 phase has been discomposed at the end of charge. Accordingly, it is speculated that the main electrochemical reaction pathway during discharge/charge processes have been replaced by the reversible formation/decomposition of LiOH. The involved reaction mechanism can be expressed by Eq. 4:

$$4Li^+ + 4e^- + O_2 + 2H_2O \leftrightarrow 4LiOH \left(E^\Theta = 3.39\,V\,vs.\,Li^+/Li\right) \quad (4)$$

Obviously, due to moisture participation, this new reaction pathway leads to the unfavorable charging voltage profiles with step-wise rise (Fig. 4a). The soluble HO_2^- and H_2O_2 have been formed with the presence of water during discharge, resulting in a lower platform during the initial charge due to their decomposition [18]. Subsequently, the discharge reaction path has been changed to the generation of LiOH, which is accompanied by the decomposition of LiOH and the rise of charge platform during the charging process. Meanwhile, the charge process may be accompanied by the decomposition of the electrolytes and by-products produced by water, resulting in the voltage elevation. Furthermore, the inevitable corrosion of Li metal anode under high-humidity conditions would result in the rapid battery failure. By contrast, the protected Li-O_2 battery, strengthened with a protective layer on the surface of Li anode, exhibits stable electrochemical performance under humid atmosphere, even at RH of 68%. As shown in Fig. 4b, the protected Li-O_2 battery exhibits an increase in overpotential during the initial cycle in dry atmosphere, which can be attributed to the increased interfacial impedance caused by the protective layer. Under humid conditions, the end-of-charge voltage in the first cycle of the protected Li-O_2 battery is reduced compared to that of the pristine Li-O_2 battery. Additionally, under high humidity (RH = 68%), the protected Li-O_2 battery exhibits a single charge plateau, whereas the unprotected battery displays three charge plateaus, indicating that the protective layer can suppress the side reactions involving water. Notably, the newly-formed protective layer consists of a large amount of alkyl and phenyl groups with hydrophobic characteristics, which can be able to hinder the

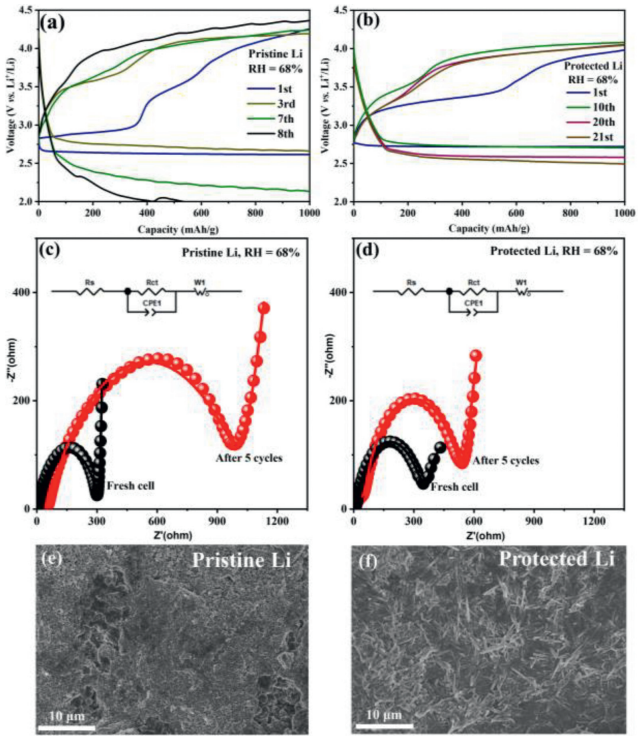

Fig. 5. Discharge/charge profiles of the Li-O_2 batteries in different cycles with the (a) pristine Li anode and (b) protected Li anode in humid O_2 atmosphere at RH = 68%. EIS of the Li-O_2 batteries at the open-circuit voltage stage and after the 5th cycle in humid O_2 atmosphere at RH = 68%: (c) the pristine Li anode and (d) the protected Li anode. Inserts are the corresponding equivalent circuit diagrams. SEM images of the Li anode in Li-O_2 batteries after 5 cycles in the humid O_2 atmosphere at RH = 68%: (e) the pristine Li anode and (f) the protected Li anode.

attack of moisture towards Li anode even under high humidity conditions.

With the aim to demonstrate the enhanced reversibility of the protected Li anode against moisture ingress, the electrochemical performance of Li-O_2 batteries with the pristine and protected Li anode are tested in humid O_2 atmosphere at the RH of 68%. The operating environment of the batteries is present in Fig. S7 (Supporting information). The cycling performance is evaluated within a voltage range of 2.0–4.5 V at a current density of 200 mA/g with a limited specific capacity of 1000 mAh/g. As shown in Fig. 5a, in addition to the detrimental step-wise charging curves, an apparent capacity decline is observed from the 7^{th} cycle for the unprotected Li-O_2 battery with the pristine Li anode, indicating the severe polarization of the battery. The poor cycling performance of Li-O_2 battery under humid condition could result from the serious corrosion of Li metal anode and the formation of LiOH byproduct derived from moisture invasion. By contrast, the Li-O_2 battery with the protected Li anode delivers an endurable electrochemical performance under moist atmosphere including a stable discharge/charge voltage plateau at 2.7/3.4 V during the initial cycle and a laudable cycle life of 210 h (21 cycles) (Fig. 5b). The admirable cycling performance with stable discharge/charge platform for the protected Li-O_2 battery could be attributed to the critical effects of ibuprofen-based protective layer to resist water and protect the Li anode from deterioration caused by water corrosion. Additionally, it can be demonstrated that the Li-O_2 battery with the protected Li anode presents the stable operation at high current density (1000 mA/g) in humid atmosphere (Fig. S8 in Supporting information). The comparison on electrochemical impedance spectra (EIS) can further confirm the superior interfacial stability between protected Li anode and pristine Li anode in the humid atmosphere (Figs. 5c and d). Utilizing the equivalent circuit in the inset, the measured data (depicted as circles) can be well fitted with the simulated curve (represented by a line), and all the resistance parameters in the equivalent circuit are provided in Table S1 (Supporting information). For the unprotected Li-O_2 battery using the pristine Li anode, the ohmic resistance (R_s) increases obviously from 5.0 Ω to 46.9 Ω and the charge-transfer resistance (R_{ct}) increases dramatically from 306.8 Ω to 1003.0 Ω after 5 cycles, mainly ascribed to severe Li corrosion. As for the Li-O_2 battery with the protected Li anode, both R_s and R_{ct} values are slightly higher than the unprotected Li-O_2 battery before cycling, probably due to the inferior conductivity of the protective layer, which is consistent with the electrochemical performance. Fortunately, the increase of charge-transfer resistance has been effectively mitigated upon cycling (Fig. 5d and Table S1), which could be attributed to the water-defendable property of the protective layer ensuring reversible redox behavior at the Li anode. Moreover, Figs. 5e and f present the surface morphologies of Li anode after 5 cycles (50 h) at the RH of 68%. The smooth surface of the pristine Li anode (Fig. 1b) has been evolved to rough surface (Fig. 5e), whereas the protected Li anode exhibits textured surface morphology before (Fig. 1c) and after cycling (Fig. 5f). After cycling in humid O_2 atmosphere, the sole LiOH product can be soundly verified by XRD results for the pristine Li anode, and severe corrosion of Li metal can even be clearly observed through optical photograph (Fig. S9 in Supporting information). By contrast, the chemical stability has been significantly improved for protected Li metal. Furthermore, the characteristic peaks associated with unique ibuprofen structure are still clearly visible in FTIR spectra of the protected Li anode after cycling (Fig. S10 in Supporting information), indicating the favorable stability of the protective layer upon repeated electrochemical processes. Due to the residual electrolytes and a small number of by-products on the surface of the protective layer after cycling, the position and intensity of the infrared peak can be changed slightly. Fortunately, the molecular structure of the protective layer has not been affected. Accordingly, it can be concluded from the above experimental results that the *in-situ* fabricated ibuprofen-based protective layer with favorable hydrophobicity and stability is able to ensure the water-defendable Li anode, subsequently, the implementation of Li-O_2 battery can be achieved in the humid atmosphere (even at RH = 68%) with a decent cycle life.

In conclusion, a uniform protective layer has been *in-situ* fabricated through chemical reaction between ibuprofen and metallic Li to achieve a water-proof Li anode for the stable operation of Li-O_2 battery in humid atmosphere. Owing to the hydrophobic property of ibuprofen-based layer (H_2O contact angle is 127°), the protected Li anode manifests the significantly enhanced moisture tolerance when it is exposed to humid atmosphere. Additionally, the favorable stability and integrity of this protective layer upon cycles ensures the reversible redox behaviors at the Li anode. As a consequence, the Li-O_2 battery using the protected Li anode is able to deliver a decent cycling lifetime of 210 h (at the limited capacity of 1000 mAh/g and a current density of 200 mA/g) even under harsh condition with a relative humidity (RH) of 68%. This facile and efficient strategy of surface hydrophobic decoration for water-tolerant Li anode offers a new avenue to the prevailing application of Li-air battery under ambient conditions.

Declaration of competing interest

The authors declare that they have no known competing financial interests or personal relationships that could have appeared to influence the work reported in this paper.

Acknowledgment

This work was financially supported by National Natural Science Foundation of China (No. 22075171).

Supplementary materials

Supplementary material associated with this article can be found, in the online version, at doi:10.1016/j.cclet.2023.108586.

References

[1] J. Yi, S. Guo, P. He, et al., Energy Environ. Sci. 10 (2017) 860–884.
[2] X. Wu, X. Wang, Z. Li, et al., Nano Lett. 22 (2022) 4985–4992.
[3] H. Zhang, J. Chen, Y. Hong, et al., Nano Lett. 22 (2022) 9972–9981.
[4] Z. Li, S. Zhou, X. Wu, et al., Adv. Funct. Mater. 33 (2023) 2211774.
[5] X. Wu, B. Niu, H. Zhang, et al., Adv. Energy Mater. 13 (2023) 2203089.
[6] X.Y. Liu, Y.Z. Fang, P.C. Liang, et al., Chin. Chem. Lett. 32 (2021) 2899–2903.
[7] L. Yan, Y.E. Qi, X. Dong, et al., eScience 1 (2021) 212–218.
[8] Y. Liu, J. Cai, J. Zhou, et al., eScience 2 (2022) 389–398.
[9] K. Wu, J. Cui, J. Yi, et al., ACS Appl. Mater. Interfaces 14 (2022) 34612–34619.
[10] K. Wu, S.K. Zhan, W. Liu, et al., ACS Appl. Mater. Interfaces 15 (2023) 6839–6847.
[11] D.G. Kwabi, T.P. Batcho, S. Feng, et al., Phys. Chem. Chem. Phys. 18 (2016) 24944–24953.
[12] P. Tan, W. Shyy, T.S. Zhao, et al., Appl. Energy 182 (2016) 569–575.
[13] S. Ma, J. Wang, J. Huang, et al., J. Phys. Chem. Lett. 9 (2018) 3333–3339.
[14] F. Wang, X. Li, ACS Omega 3 (2018) 6006–6012.
[15] Z.Z. Shen, S.Y. Lang, C. Zhou, et al., Adv. Energy Mater. 10 (2020) 2002339.
[16] A. Dai, Q. Li, T. Liu, et al., Adv. Mater. 31 (2019) 1805602.
[17] Z. Guo, X. Dong, S. Yuan, et al., J. Power Sources 264 (2014) 1–7.
[18] Y. Qiao, S. Wu, J. Yi, et al., Angew. Chem. Int. Ed. 56 (2017) 4960–4964.
[19] N.B. Aetukuri, B.D. McCloskey, J.M. García, et al., Nat. Chem. 7 (2015) 50–56.
[20] F. Li, S. Wu, D. Li, et al., Nat. Commun. 6 (2015) 7843.
[21] S. Huang, Z. Cui, N. Zhao, et al., Electrochim. Acta 191 (2016) 473–478.
[22] Z. Li, Y.E. Liu, S. Weng, et al., Energy Stor. Mater. 58 (2023) 94–100.
[23] L. Qin, D.Y. Zhai, W. Lv, et al., J. Nano Energy Power Res. 40 (2017) 258–263.
[24] H. Deng, Y. Qiao, S.C. Wu, et al., ACS Appl. Mater. Interfaces 11 (2019) 4908–4914.
[25] Z.Y. Guo, X.L. Dong, Y.G. Wang, et al., Chem. Commun. 51 (2015) 676–678.
[26] T. Zhang, J. Yang, J.H. Zhu, et al., Chem. Commun. 54 (2018) 1069–1072.
[27] S. Wu, K. Zhu, J. Tang, et al., Energy Environ. Sci. 9 (2016) 3262–3271.
[28] J. Hassoun, H.G. Jung, D.J. Lee, et al., Nano Lett. 12 (2012) 5775–5779.
[29] J. Yi, K. Liao, C. Zhang, et al., ACS Appl. Mater. Interfaces 7 (2015) 10823–10827.
[30] J. Amici, M. Alidoost, C. Francia, et al., Chem. Commun. 52 (2016) 13683–13686.
[31] T. Liu, J.T. Frith, G. Kim, et al., J. Am. Chem. Soc. 140 (2018) 1428–1437.
[32] S.C. Wu, K. Zhu, J. Tang, et al., Energy Environ. Sci. 9 (2016) 3262–3271.
[33] B.G. Kim, J.S. Kim, J. Min, et al., Adv. Funct. Mater. 26 (2016) 1747–1756.
[34] J.J. Xu, Q.C. Liu, Y. Yu, et al., Adv. Mater. 29 (2017) 6.
[35] J.J. Wang, X.W. Chen, Y.F. Ke, et al., Electrochim. Acta 424 (2022) 140623.
[36] B. Han, Y. Zou, R. Ke, et al., ACS Appl. Mater. Interfaces 13 (2021) 21467–21473.
[37] S. Li, Y. Huang, W. Ren, et al., Chem. Eng. J. 422 (2021) 129911.
[38] T. Liu, X. l. Feng, X. Jin, et al., Angew. Chem. Int. Ed. 58 (2019) 18240–18245.
[39] S. Wu, J. Yi, K. Zhu, et al., Adv. Energy Mater. 7 (2017) 1601759.
[40] K. Liao, S. Wu, X. Mu, et al., Adv. Mater. 30 (2018) e1705711.
[41] C. Li, J. Wei, K. Qiu, et al., ACS Appl. Mater. Interfaces 12 (2020) 23010–23016.
[42] W. Liang, F. Lian, N. Meng, et al., Energy Stor. Mater. 28 (2020) 350–356.
[43] X. Zou, K. Liao, D. Wang, et al., Energy Stor. Mater. 27 (2020) 297–306.
[44] H. Dong, Y. Wang, P. Tang, et al., J. Colloid Interface Sci. 584 (2021) 246–252.
[45] Y. Ma, P. Qi, J. Ma, et al., Adv. Sci. 8 (2021) 2100488.
[46] T.N. Hsia, H.C. Lu, Y.C. Hsueh, et al., J. Colloid Interface Sci. 626 (2022) 524–534.
[47] J. Lei, Z. Gao, L. Tang, et al., Adv. Sci. 9 (2022) 2103760.
[48] R. Li, Y. Fan, C. Zhao, et al., Small Methods 7 (2023) 2201177.
[49] W.L. Bai, Z. Zhang, X. Chen, et al., Chem. Commun. 56 (2020) 12566–12569.
[50] Z. Fu, Z. Wei, X. Lin, et al., Electrochim. Acta 78 (2012) 195–199.
[51] J. Li, L.F. Hou, L.H. Luan, et al., Int. J. Electrochem. Sci. 16 (2021) 210749.
[52] Z. Li, Z. Gong, X.Y. Wu, et al., Chin. Chem. Lett. 33 (2022) 3936–3940.
[53] S.S. Braga, I.S. Goncalves, E. Herdtweck, et al., New J. Chem. 27 (2003) 597–601.
[54] J. Zhou, C. Liao, X. Feng, et al., J. Instrum. Anal. 23 (2004) 18–21.
[55] A. Hagopian, M.L. Doublet, J. S. Filhol. Energy Environ. Sci. 13 (2020) 5186–5197.
[56] X. Xu, S. Wang, H. Wang, et al., J. Energy Chem. 27 (2018) 513–527.
[57] L. Chen, L.L. Shaw, J. Power Sources 267 (2014) 770–783.
[58] X.B. Cheng, H.J. Peng, J.Q. Huang, et al., Small 10 (2014) 4257–4263.
[59] R.R. Miao, J. Yang, X.J. Feng, et al., J. Power Sources 271 (2014) 291–297.
[60] M. Zier, F. Scheiba, S. Oswald, et al., J. Power Sources 266 (2014) 198–207.
[61] X.B. Cheng, Q. Zhang, J. Mater. Chem. 3 (2015) 7207–7209.
[62] C.T. Love, O.A. Baturina, K.E. Swider-Lyons, ECS Electrochem. Lett. 4 (2015) A24–A27.